Coupled thermo-mechanics of single-wall carbon nanotubes

F Scarpa* and H X Peng†

Advanced Composites Centre for Innovation and Science,

University of Bristol, BS8 1TR Bristol, UK

L Boldrin‡ and C D L Remillat§

Department of Aerospace Engineering,

University of Bristol, BS8 1TR Bristol, UK

S Adhikari¶

Multidisciplinary Nanotechnology Centre,

University of Swansea, SA2 8PP Swansea, UK

arXiv:1008.5098v1 [physics.atm-clus] 30 Aug 2010

Abstract

The temperature-dependent transverse mechanical properties of single-walled nanotubes are studied using a molecular mechanics approach. The stretching and bond angle force constants describing the mechanical behaviour of the sp^2 bonds are resolved in the temperature range between 0 K and 1600 K, allowing to identify a temperature dependence of the nanotubes wall thickness. We observe a decrease of the stiffness properties (axial and shear Young's modulus) with increasing temperatures, and an augmentation of the transverse Poisson's ratio, with magnitudes depending on the chirality of the nanotube. Our closed-form predictions compare well with existing Molecular Dynamics simulations.

*Electronic address: f.scarpa@bristol.ac.uk

†Electronic address: h.x.peng@bristol.ac.uk

‡Electronic address: l.boldrin@bristol.ac.uk

§Electronic address: c.remillat@bristol.ac.uk

¶Electronic address: s.adhikari@swansea.ac.uk

Carbon nanotubes-based composites, both based on metal/ceramics [1], or polymer matrix [2], undergo substantial thermal loading during both the manufacturing phase and their operational life. This specific aspect of their multifunctional behaviour has generated a substantial amount of activity in the identification of the thermal properties of nanotubes, with particular emphasis on the thermal conductivity [3–7]. The dependence of the Young's modulus and tensile strength of single-walled carbon nanotubes (SWCNTs) has been investigated using various MD techniques [8–11] and hybrid atomistic-Finite Element techniques [12, 13]. The importance of the interplay between the nanotube and the polymer matrix during different environmental temperatures has been highlighted by Wei from Monte Carlo/Molecular Dynamics (MC/MD) simulations on a periodic assembly of a PE-(19,0) CNT nanocomposite [14]. The use of simulations to predict the temperature dependence of the nanotubes mechanical properties is a necessity, because of the difficulties involved in obtaining direct experimental measurements in different thermal environments. However, all the predictive tools so far available to simulate and design the stiffness of CNT-based composites are not based on analytical formulas that would facilitate the work of the material scientist and engineer. The existing atomistic-continuum models describing the elastic properties of carbon nanotubes in closed form [15, 16] have their bonds force constant formulated only for room temperature. In this work we propose a compact formulation that express the relation between the sp^2 C-C bond force constants and the surrounding temperature of the nanotube, providing a functional description of the coupled thermal and mechanical linear elastic properties of SWCNTs.

In the following description of the model, we will use the suffix ^{T} to indicate the temperature-dependent force constants, while the suffix ^{o} will indicate a force constant term referred to the room temperature ($T_0 = 300\,K$). Adopting in part the Universal Force Field (UFF) nomenclature [17], the stretching force constant related to the calculation of the harmonic harmonic potential energy associated to the stretching deformation is expressed as:

$$k_{IJ}^T = 664.12\,\frac{Z_I^* Z_J^*}{r_{IJ}^3} \tag{1}$$

Where Z_I^* and Z_J^* are the effective electronic charges (1.914 electron units). At room temperature, the equilibrium length r_{IJ}^0 between the atoms I and J is defined as $0.142\,nm$, with the stretching constant (1) assuming the value of $6.52\,10^{-7} N\,nm^{-1}$, which is consistent

with the force constant used in the AMBER model [18]. The bending force constant k^T_{IJK} related to the harmonic potential energy associated to the bond bending angle is the second partial derivative of the bending energy functional [17]:

$$k^T_{IJK} = \left(\frac{\partial^2 E_\theta}{\partial \theta^2} \right) = \frac{\overline{\beta}\, Z^*_I Z^*_K}{r^5_{IK}}\, r_{IJ}\; r_{JK} \left\{ 3\, r_{IJ}\, r_{JK} \left[1 - (\cos\theta)^2 \right] - r^2_{IK}\, \cos\theta \right\} \tag{2}$$

Where the distance between the atoms I and K is expressed as $r_{IK} = r^2_{IJ} + r^2_{JK} - 2\, r_{IJ}\, r_{JK} \cos\theta$. At room temperature, the bond angle is equal to $\theta = 120\, C^o$. The term $\overline{\beta}$ is equal to $332.6/r_{IJ}/r_{jk}$ to obtain at room temperature a value of k^T_{IJK} consistent with the one provided by the AMBER force, and used by several authors in atomistic-continuum mechanics models ($8.76\, 10^{-10}\, N\, nm/rad^2$). The torsional potential energy between bonds IJ and KL is approximated as the summation of three cosine Fourier terms based on ω (the angle between the IL axis and the IJK plane):

$$E_\omega = K^T_{IJKL} \sum_{n=0}^{2} C_n \cos n\omega_{IJKL} \tag{3}$$

At room temperature the constant K^T_{IJKL} is assumed equal as $2.78\, 10^{-10} N/nm/rad^2$, consistent with the value used by several Authors [19, 20]. Due to the very low sensitivity of the torsional constant versus the temperature, in our model we consider the term K^T_{IJKL} as constant with the different thermal environments, and will be indicated as K^0_{IJKL} in the rest of the work. Following Chen *et al* [13], the bond angle θ is also assumed constant at the room temperature value ($\theta_0 = 2\,\pi/3$). The thermal dependence of the force constants (1) and (2) is provided by the thermal variation of the bond length through an equivalent coefficient of thermal expansion (CTE) α:

$$r_{IJ} =^0 r_{IJ}\, (1 + \alpha\, \Delta T) \tag{4}$$

Where $\Delta T = T - T_0$. In this work, we consider as CTE for the bond the coefficient of thermal expansion of suspended graphene sheets calculated using a non-uniform Green's function approach by Jiang *et al* [21]. At room temperature, the coefficient of thermal expansion is equal to -6 X $10^{-6}\, K^{-1}$, 14 % lower than the experimental value measured by Bao *et al* [22]. The CTE assumes a value of -3.2 X $10^{-6}\, K^{-1}$ at 20 K, to decrease to a minimum of -1.25 X $10^{-6}\, K^{-1}$ at ~ 80 K. After this temperature, the coefficient of thermal expansion increases monotonically, although it remains negative up to 650 K. At

$T = 1550\,K$, α brings a value of 5.0 X $10^{-6}\,K^{-1}$. Assuming $r_{IJ} = r_{JK}$, using (4) in (1) and (2), it is possible to express the harmonic potentials related to the stretching and bending energy respectively with the variation of the environmental temperature.

The equivalent mechanical behaviour of the C-C bond is represented at this stage by equating the harmonic potentials with the correspondent strain energies deformations under axial, bending and torsion of a structural beam element [19]:

$$\frac{k_{IJ}^T}{2}(\Delta r)^2 = \frac{EA}{2\,r_{IJ}}(\Delta r)^2,\ \frac{K_{IJKL}^T}{2}(\Delta\varphi)^2 = \frac{GJ}{2\,r_{IJ}}(\Delta\varphi)^2,\ \frac{k_{IJK}^T}{2}(\Delta\theta)^2 = \frac{EI}{2\,r_{IJ}}\frac{4+\Phi}{1+\Phi}(\Delta\theta)^2 \tag{5}$$

In (5), E and G are the equivalent Young's and shear modulus of the material representing the C-C bond, $I = \pi\,d^4/32$ is the polar inertia moment of the bond beam (considered having a circular cross-section of diameter d, equal to the thickness). Differently from other approaches used in open literature [23], we adopt in (5) a Timoshenko beam having deep shear cross-deformation behaviour as representative beam model, to consider more realistic distributions of thickness and equilibrium length existing in graphene and nanotubes [24–27]. The effect due to the shear-induced cross section deformation is provided by the constant $\Phi = 12EI/G/A_s/r_{IJ}^2$ [26, 28], where $A_s = \pi d^2/4/F_s$ is the reduced cross section of the beam by the shear correction term F_s depending on the Poisson's ratio ν of the equivalent C-C bond material [29]:

$$F_s = \frac{6 + 12\nu + 6\nu^2}{7 + 12\nu + 4\nu^2} \tag{6}$$

The equivalence between the harmonic potentials and the beam strain energies in (5) leads to the following set of equations:

$$E = \frac{4\,k_{IJ}^T r_{IJ}}{\pi\,d^2},\ G = \frac{32\,K_{IJKL}^T r_{IJ}}{\pi\,d^4},\ k_{IJK}^T = EI\frac{4+\Phi}{r_{IJ}(1+\Phi)} \tag{7}$$

Inserting (6) into the definition of the shear constant Φ, and solving for E in (7), we obtain the following nonlinear expression in d and ν for a specific temperature T:

$$k^T_{IJK} = \frac{\pi\, k^T_{IJ}\, d^2 \left(448\,\pi^2 K^T_{IJKL}\, r^2_{IJ} + 384\,\pi^2 K^T_{IJKL}\, r^2_{IJ}\,\nu + 9\,k^T_{IJ}\pi^2 d^4\nu + 9k^T_{IJ}\pi^2 d^4\right)}{16\,\pi\,(112\,\pi^2 r^2_{IJ}\, K^T_{IJKL} + 96\pi^2 r^2_{IJ}\, K^T_{IJKL}\nu + 9\,k^T_{IJ}\pi^2 d^4\nu + 9k^T_{IJ}\pi^2 d^4)} \tag{8}$$

We impose the additional condition that the equivalent material of the C-C bond beam behaves as *isotropic*, i.e., with no directional preference in its mechanical response. The isotropic condition $G = E/2/\,(1+\nu)$, together with relation (8) constitutes a system of nonlinear equations which can be solved with traditional methods, such as the Marquardt algorithm. The solution of the system yields a unique value of the thickness d for a given temperature T. At room temperature, the thickness identified using this approach yields a value of 0.084 nm, equal to the one found for single wall and nanotube bundles in [25]. We observe a low sensitivity of the thickness corresponding to the isotropic condition versus the temperature, with a minimum value of 0.0835 nm at 1600 K, and a maximum value of 0.0841 nm for $T = 470\,K$. The temperature dependence of the thickness can be described using a polynomial curve of the 9^{th} order, as shown in Table I. It is interesting to notice that the C-C bond behaves mechanically as if made of a quasi-zero Poisson's ratio behaviour, like in natural-occurring cork [30]. The 0.084 nm value at room temperature is also consistent with the 0.084 nm found by Kudin *et al* [31], and 0.074 nm identified by Tu and Ou-Yang [32]. From simulations using the MM3 potential, Batra and Sears have found an equivalent thickness of 0.043 nm for different chiral configurations [33], although a value of 0.1 nm was observed in nanotubes undergoing bending and breathing vibration modes [34]. Zhang and Shen identify thickness of 0.088 nm and 0.087 nm for (17,0) and (21,0) nanotubes respectively, while for (10,10) and (12,12) the thickness calculated is 0.067 nm [10]. The thickness values calculated with our method do compare well with the 0.080 nm of Chen and Cao [35], although they are higher than the 0.066 nm of Yakobson *et al* [36], and 0.60 nm of Vodenitcharova and Zhang [37].

Classical mechanistic theories for the elastic properties of single-wall carbon nanotubes consider the strain energy associated to the deformation of sp^2 bonds in terms of stretching and bond angle constants (C_ρ and C_θ respectively [15, 16]). For the bond angle constant (moment), we consider that for linear elasticity the lattice is dominated by hinging deformation [38]. In cellular structures under general flexural/axial deformations, the hinging constant can be calculated as $C_\theta = EI/q$, where q is the portion of the C-C bond length undergoing hinging, while the segment $r_{IJ} - q$ deforms as a rigid body ([39], see also Figure 1). Using

the relations (7), the bending angle constant can be rewritten as $C_\theta = k_{IJ}^T d^2 r_{IJ}/16/q$. Considering a ratio $r_{IJ}/q = 5$, inserting the numerical values of the thickness and equilibrium length at room temperature we obtain a value of 1.44 $nN\,nm\,rad^{-2}$, well in line with the 1.42 $nN\,nm\,rad^{-2}$ used in [15, 16]. The stretching constant is calculated as $C_\rho = k_\rho\, k_{IJ}^T$, where $k_\rho = 1.128$ to converge to the 0.36 $TPa\,nm^{-1}$ of the in-plane graphitic surface modulus (chiral index $n \to \infty$) [38, 40]. At room temperature, the stretching constant identified in this model is equal to 735 $nN\,nm^{-1}$, which compares well with the 742 $nN\,nm^{-1}$ used by Shen and Li [16]. Cadelano *et al [41]* have identified a value of the surface modulus of graphene-type systems equal to 0.312 $TPa\,nm^{-1}$ at zero temperature damped dynamics using tight binding calculations and continuum elasticity. Using our approach, we observe a value of 0.332 $TPa\,nm^{-1}$ at zero temperature, 6 % higher. For both the bending and stretching constants, we observe a very low dependence versus the environmental temperature between $370\,K < T < 570\,K$. The stretching constant then decreases with increasing temperatures with an approximate rate of 0.015 $nN\,nm^{-1}K^{-1}$, a behaviour similar to the one of the C_θ constant, having the latter a decrease rate of $4.9\,10^{-5}\,nN\,nm\,rad^{-2}K^{-1}$ between 600 K and 1600 K. At low temperatures, both the force and bending constants decrease from values equal to 99.2 % of the maximum C_θ and C_ρ at 1 K to a minimum at 70 K corresponding to the 98.6 % of the maximum of the constants at 450 K. Similarly to the C-C bond thickness, the force stretching and bending constants can be expressed in polynomial terms, as illustrated in Table I.

The temperature-dependent constants C_ρ and C_θ can now be used in atomistic-continuum approaches illustrated in open literature to model in a closed-form solution the mechanical properties of SWCNTs under different temperature conditions. In this work we have used the formulation proposed by Shen and Li [16] to simulate the axial and shear stiffness, as well as the Poisson's ratio of the nanotubes with armchair and zigzag geometry. We compare the surface Young's modulus Y_{11}^s calculated in analytical form against the results obtained through MD simulations using a REBO potential by Zhang and Shen [10] (Figure 2). Our predictions are well in line with the 0.352 $TPa\,nm^{-1}$ of Tu and Ou-Yang [32] and Pantano *et al* [42], although 3.5 % higher than Li and Chou [19] and Wang and co-Authors [43]. In terms of longitudinal modulus Y_{11}^l (defined as Y_{11}^s/d), our predictions tend to overestimate the MD simulations in [10]. For example, our axial moduli for (17,0) nanotubes are 9 % higher than the molecular dynamics simulations at $T = 300\,K$, while a at a temperature of 1000 K our

overestimate is around 11 %. The effective Young's modulus $Y_{11} = Y_{11}^s / (R/2)$(where R is the diameter of the nanotube) has been also derived by Hsieh *et al* [11] from the vibration amplitude of $(n, 0)$ clamped-free nanotubes simulated with a Tersoff-Brenner potential at temperatures ranging between 0 K and 2000 K. The MD simulations in [11] are least-squares fitted to an asymptotic value of the graphene Young's modulus equal to 1.2 TPa found by [44, 45] at a not specified temperature, 20 % higher than the experimental value found by Lee *et al* for a thickness of 0.34 nm [46]. A general comparison of the results from [11] against our simulations is presented in Figure 3, showing a general agreement between trends related to the nanotube radius at $T = 1100\,K$, and within the temperature range 50 K - 1100 K. We observe a good convergence between MD and our simulations especially for CNT radius lower than 0.5 nm, and excellent agreement (percentage error less than 4 %) for (7,0) SWCNTs over the temperature range considered. Hsieh and co-Authors record a steep decrease in terms of axial stiffness above 1100 K, corresponding to an abrupt change of the standard deviation associated to the dynamic tip displacements of the tube [11]. We observe also an overestimate for the shear modulus G_{12} [10], with discrepancies around 29 % and 28 % at 1000 K and 1200 K respectively. However, our predictions show a decrease of the longitudinal shear modulus versus the temperature, opposite from the results derived in [10]. The transverse Poisson's ratio ν_{21} increases with the temperature (Figure 4), although the augmentation is limited on average to a 3 % increase between $T = 300\,K$ and $T = 1200\,K$ for the different chirality and tube diameters. The low sensitivity of the Poisson's ratio over the temperature is due to the weak dependency versus the temperature itself of the term $C_\rho r_{IJ}^2 / C_\theta$, which is contained both in the numerator and denominator of the Poisson's ratio expression [16]. Chen *et al.* [13] observe also an increase of ν_{21} with temperature (31 % of increase for zizgag tubes of 1.2 nm diameter between room temperature and $T = 1200\,K$). The discrepancy between theirs and our predictions is due mainly to the coefficient of thermal expansion used for the C-C bond, being positive in their case for $T > 298\,K$, while our model has a positive CTE for temperatures higher than 650 K [21]. We observe that Zhang and Shen predict a transverse Poisson's ratio for a (17,0) nanotube at $T = 300\,K$ equal to 0.17, in good agreement with our value of 0.16 [10]. We note that for graphene-type systems, our model predicts at zero temperature a Poisson's ratio of 0.12, significantly lower than the 0.31 identified in [41]. However, our range of Poisson's ratios at room temperature for zigzag tubes (Figure 4) is in line with the 0.12 - 0.19 values predicted by Sanchez-Portal *et*

al [47], the 0.15 of Kudin and co-Authors [31], 0.21 of Sears and Batra [48], and 0.24 from Zhou *et al* [49].

In summary, our model allows to predict in a compact form the overall elastic transverse properties of single wall nanotubes over a large temperature range. The bending and stretching constants identified with our approach capture the intrinsic hinging/stretching behaviour of sp^2 C-C bonds in nanotubes, and relate the stiffness and Poisson's ratio to the ambient temperature of the nanotube, with 2 % average decrease of the Young's modulus between the ambient temperature and 1200 K for a given tube chirality.

[1] Zhan, Guo-Dong, Kuntz, Joshua D., Wan, Julin, and Mukherjee, Amiya K., Nature Materials **1**, 38 (2003).

[2] M. J. Biercuk, M. C. Llaguno, M. Radosavljevic, J. K. Hyun, A. T. Johnson, and J. E. Fischer, Applied Physics Letters **80**, 2767 (2002).

[3] Jianwei Che, Tahir Cagin, and William A Goddard III, Nanotechnology **11**, 65 (2000).

[4] J. Hone, M.C. Llaguno, M.J. Biercuk, A.T. Johnson, B. Batlogg, Z. Benes, and J.E. Fischer, Applied Physics A **74**, 339 (2002).

[5] Sun C Q, Bai H L, Tai B K, Li S, and Jiang E Y, J. Phys. Chem.B **107**, 7544 (2003).

[6] Kwon Y and Berber S and Tomanek D, Physical Review Letters **92**, 01590 (2004).

[7] Cao G and Chen X and Kysar GW, Journal of the Mechanics and Physics of Solids **54**, 1206 (2006).

[8] C. Wei, K. Cho, and D. Srivastava, Phys. Rev. B **67**, 115407 (2003).

[9] T. Dumitrica, M. Hua, and B. I. Yakobson, Proceedings of the National Academy of Sciences of the United States of America **103**, 6105 (2006), ISSN 00278424.

[10] Zhang CL and Shen HS, Applied Physics Letters **89**, 081904 (2006).

[11] Hsieh JY, Lu JM, Huang MY, and Hwang CC, Nanotechnology **17**, 3920 (2006).

[12] Liu TT and Wang X, Physics Letters A **365**, 144 (2007).

[13] Chen X, Wang X, and Liu BY, Journal of Reinforced Plastics and Composites **28**, 551 (2009).

[14] C. Wei, Applied Physics Letters **88**, 093108 (pages 3) (2006).

[15] Chang T and Gao H, J. Mech. Phys. Solids **51**, 1059 (2003).

[16] Shen L and Li J, Physical Review B **89**, 045414 (2004).

[17] Rappe A K, Casewit C J, Colwell K S, Goddard W A, and Skiff W M, Journal of the American Chemical Society **114**, 10024 (1992).

[18] Cornell W D, Cieplak P, Bayly C I, Gould I R, Merz K M, Ferguson D M, Spellmeyer D C, Fox T, Caldwell J W, and Kollman P A, Journal of American Chemical Society **117**, 5179 (1995).

[19] Li C and Chou TW, International Journal of Solids and Structures **40**, 2487 (2003).

[20] G. M. Odegard, T. S. Gates, K. E. Wise, C. Park, and E. J. Siochi, Composites Science and Technology **63**, 1671 (2003), ISSN 0266-3538, modeling and Characterization of Nanostructured Materials.

[21] Jiang JW and Wang JS and Li B, Physical Review B **80**, 205429 (2009).

[22] Bao W, Miao F, Chen Z, Zhang H, Jang W, Dames C, and Lau C N, Nature Nanotechnology **4**, 562 (2009).

[23] Tserpes K I and Papanikos P, Composites B **36**, 468 (2005).

[24] Huang Y, Wu J, and Hwang K C, Physical Revue B **74**, 245413 (2006).

[25] Scarpa F and Adhikari S, J. Phys. D: App. Phys. **41**, 085306 (2008).

[26] Scarpa F, Adhikari S, and Phani A S, Nanotechnology **20**, 065709 (2009).

[27] Scarpa F, Adhikari S, Gil A J, and Remillat C, Nanotechnology **21**, 125702 (2010).

[28] Przemienicki J S, *Theory of Matrix Structural Analysis* (McGraw-Hill, New York, 1968).

[29] Kaneko T, J. Phys. D: App. Phys. **8**, 1927 (1974).

[30] Gibson L J and Ashby M F, *Cellular Solids: structure and properties* (Cambridge Press, 1997), 2nd ed.

[31] Kudin K N, Scuseria G E, and Yakobson B I, Phys. Rev. B **64**, 235406 (2001).

[32] Tu Z and Ou-Yang Z, Phys. Rev. B **65**, 233407 (2002).

[33] Batra RC and Sears A, Modelling and Simulation in Materials Science and Engineering **15**, 835 (2007).

[34] Batra RC and Gupta SS, ASME Journal of Applied Mechanics **75**, 061010 (2008).

[35] X Chen and G Cao, Nanotechnology **17**, 1004 (2006).

[36] B. I. Yakobson, C. J. Brabec, and J. Bernholc, Phys. Rev. Lett. **76**, 2511 (1996).

[37] T. Vodenitcharova and L. C. Zhang, Phys. Rev. B **68**, 165401 (2003).

[38] P P Gillis, Carbon **22**, 387 (1984).

[39] Masters IG and Evans KE, Composite Structures **35**, 403 (1996).

[40] Cho J, Luo J J, and Daniel I M, Comp. Sci. Tech. **67**, 2399 (2007).

[41] E. Cadelano, P. L. Palla, S. Giordano, and L. Colombo, Phys. Rev. Lett. **102**, 235502 (2009).

[42] A. Pantano, M. C. Boyce, and D. M. Parks, Phys. Rev. Lett. **91**, 145504 (2003).

[43] L. Wang, Q. Zheng, J. Z. Liu, and Q. Jiang, Phys. Rev. Lett. **95**, 105501 (2005).

[44] Hernandez E, Goze C, Bernier P, and Rubio A, Physical Review Letters **80**, 4502 (1998).

[45] Lier G V, Alsenoy C V, Doren V V, and Greelings P, Chem. Phys. Lett. **326**, 181 (2000).

[46] Lee C, Wei X, Kysar J W, and Hone J, Science **321**, 385 (2008).

[47] D. Sánchez-Portal, E. Artacho, J. M. Soler, A. Rubio, and P. Ordejón, Phys. Rev. B **59**, 12678 (1999).

[48] A. Sears and R. C. Batra, Phys. Rev. B **69**, 235406 (2004).

[49] Z. Xin, Z. Jianjun, and O.-Y. Zhong-can, Phys. Rev. B **62**, 13692 (2000).

Quantity	p_1	p_2	p_3	p_4	p_5	p_6	p_7	p_8	p_9	p_{10}
d X 10^{-5} [nm]	-2.256	2.571	12.7	-13.6	-17.78	13.14	14.81	14.13	-23.66	8401
C_θ X 10^{12} $[N\,nm\,rad^{-2}]$	-1.84	2.181	9.427	-9.675	-14.92	12.9	12.47	-11.97	-19.8	1435
C_ρ X 10^{10} $[N\,nm^{-1}]$	-5.731	6.702	2873	-29.83	-45.55	35.13	37.83	-36.98	-59.98	7340

Table I: Polynomial interpolations for the thickness, stretching and hinging force constants for the sp^2 C-C bond lattice versus the temperature. The polynomials are of the type $y = \sum_{n=1}^{10} p_n \widehat{T}^{10-n}$, where $\widehat{T} = \left(T - \overline{T}\right)/\sigma\,(T)$, with $\overline{T} = 800\,K$ and standard deviation $\sigma\,(T) = 466\,K$. All fittings have an average R^2 of 0.991, with 95 % of confidence interval.

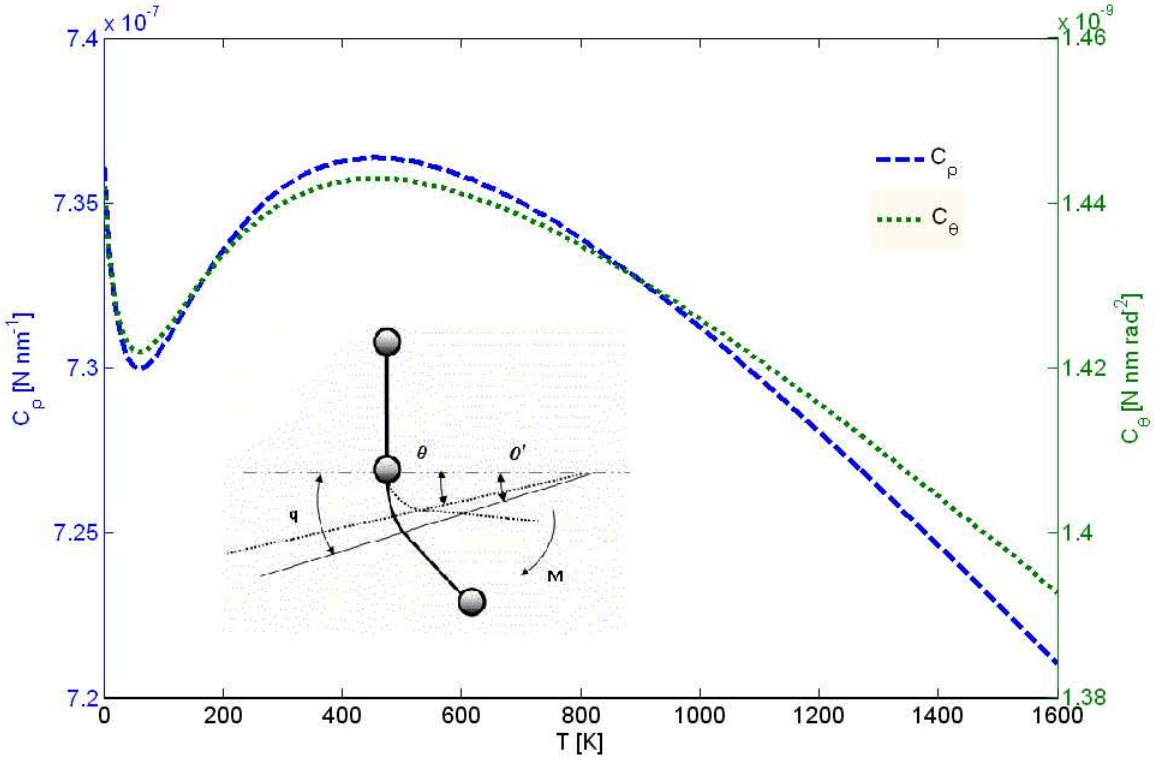


Figure 1: The variation of the stretching constant C_ρ and hinging constant C_θ over the temperature. The hinging constant is calculated considering the change in angular deformation $\theta - \theta' = \Delta\theta = \int_0^q \frac{M}{EI}\,dq = Mq/EI$. Under hinging, only the initial portion $q \simeq r_{IJ}/5$ of the bond length deforms by rotation, while the rest of the bond deforms as a rigid body [39]. The hinging constant is then defined as $C_\theta = M/\Delta\theta = EI/q$.

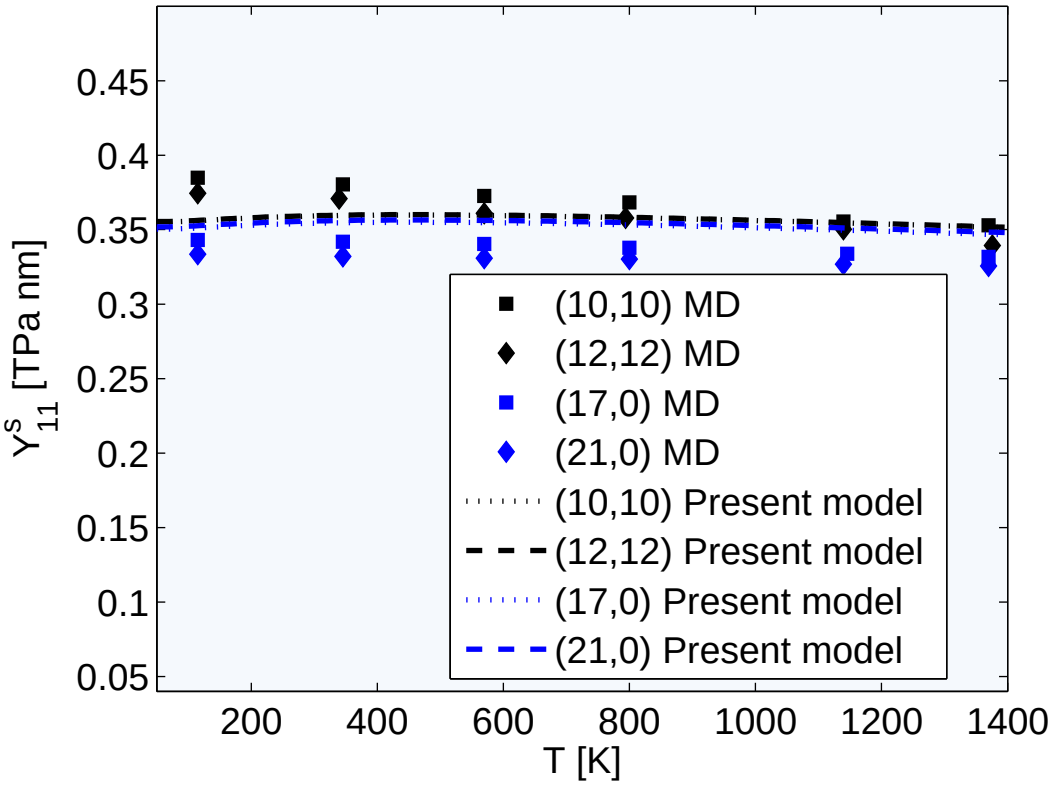


Figure 2: Comparison between the surface Young's modulus of different zigzag and armchair SWCNTs and the MD simulations from [10]

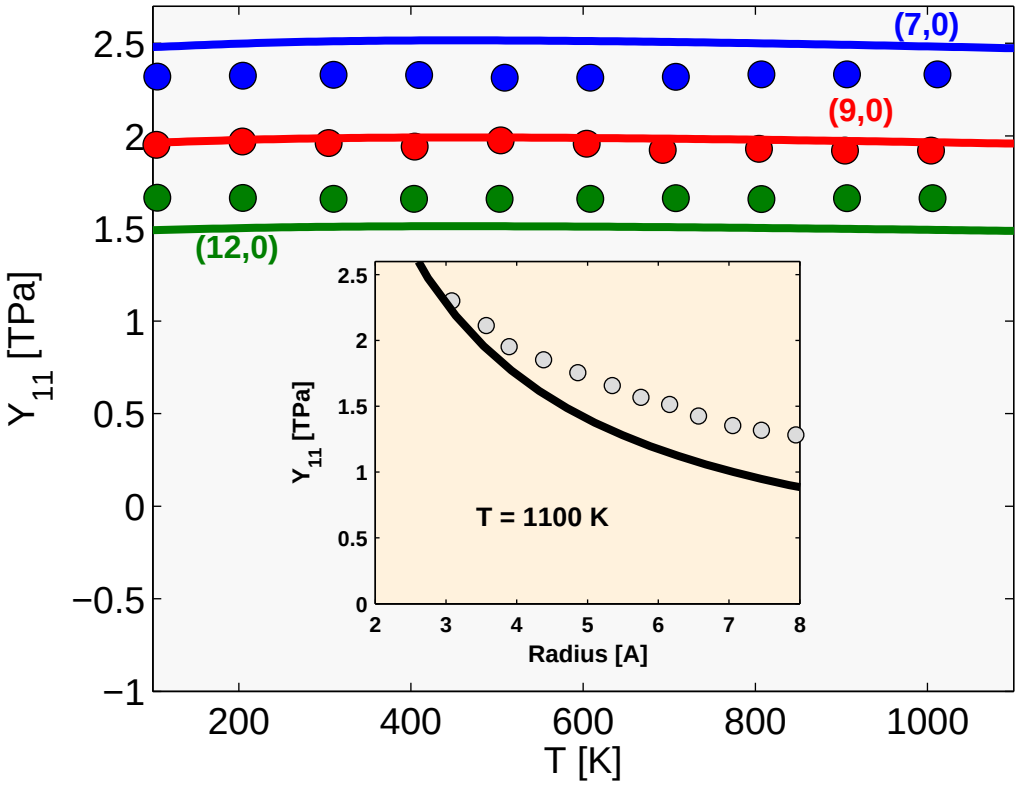


Figure 3: The effective Young's modulus modulus for $(n, 0)$ SWCNTs. The results from the proposed method (continuous line) are compared with the ones from Hsieh and co-Authors [11] (circular dots).

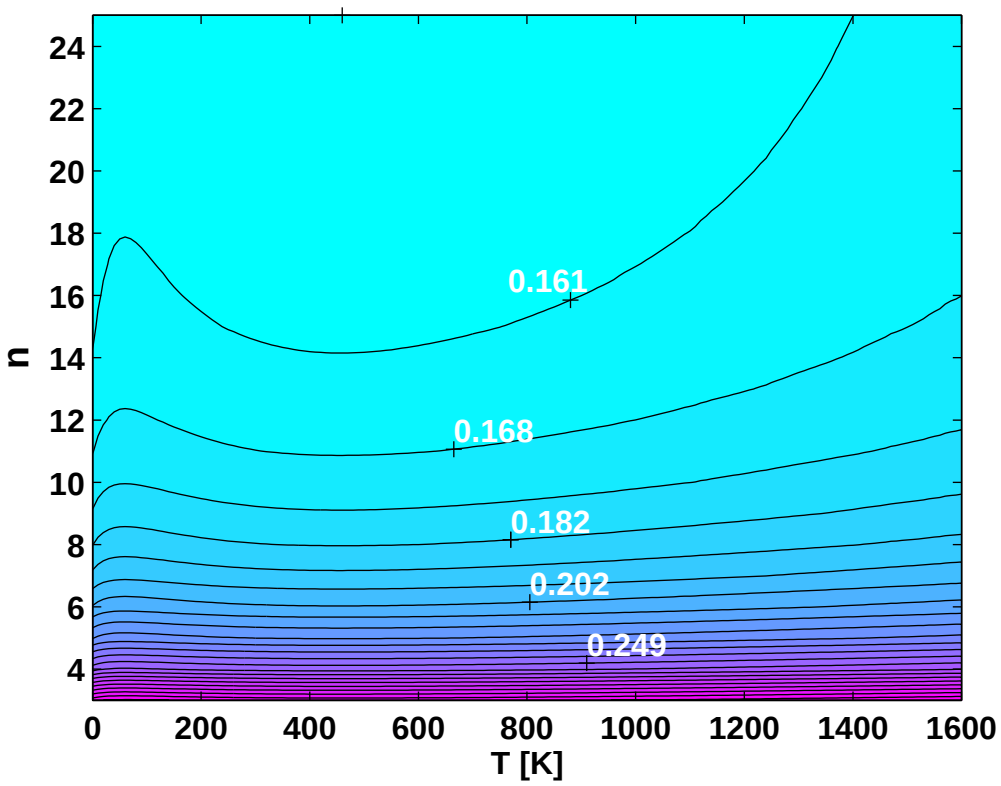


Figure 4: Map of the transverse Poisson's ratio ν_{21} for $(n, 0)$ tubes versus the the chiral index n and temperature.